

FORMATION OF IRON-RICH NANOPARTICLES WITHIN GLASSY SILICATE SPHERULES IN LUNAR SOIL. K. K. Ohtaki¹, J. P. Bradley¹, J. J. Gillis-Davis¹, G. J. Taylor¹, and H. A. Ishii¹, ¹Hawai'i Institute for Geophysics and Planetology, University of Hawai'i at Mānoa, Honolulu, HI 96822 USA (kohtaki@hawaii.edu)

Introduction: Nanophase iron (npFe⁰) particles are often observed in the rims of lunar soil grains [1–3]. Hypotheses for how they form are: condensation from solar wind-sputtered or micrometeorite impact-generated vapor [4], or segregation and reduction of higher valence Fe by solar wind irradiation [5,6]. In addition to npFe⁰ particles in the rims, nano- to micro-sized Fe-rich particles and Fe-sulfide particles have been observed in the interior of lunar soil glasses and agglutinates as well [3,7,8]. The larger opaque particles have been proposed to form via repeated heat treatments and agglomeration of nano-sized Fe particles [3] or even from impacting iron-bearing meteorites [7]. For this study, we focus on impact glass spherules that have experienced extensive melt and quench processes. We investigate the elemental distribution in the Fe-rich inclusions within these spherules and infer plausible formation routes.

Experimental: Amorphous silicate spherules in lunar soil 10084 were selected using scanning electron microscopy (SEM) and energy dispersed spectroscopy (EDS) on the University of Hawaii FEI Helios 660 dual beam focused ion beam instrument (FIB) with retractable SDD EDS detector (Oxford Instruments). According to the criteria distinguishing silicate glass of impact and volcanic origins suggested by Delano *et al.* [9], relatively large spherules (diameter>8 μm) with compositional inhomogeneity were chosen and thinned for transmission electron microscopy (TEM) analysis. FIB was used for TEM sample preparation instead of microtomy, which can result in sample loss due to blade chatter for large silicate spheres. TEM analysis was performed on the UH FEI 60-300 G2 Titan Scanning/TEM at 300 keV. Elemental distribution in the spherules was mapped using the FEI TitanX STEM at the Molecular Foundry at Lawrence Berkeley National Laboratory utilizing a four-SDD EDS system (Bruker).

Results and discussion: Fig. 1 shows the overview high-angle annular dark field (HAADF) images and EDS elemental maps of a ~10 μm diameter silicate spherule with Fe-rich inclusions with sizes of ~10-100 nm. The inclusions are distributed in a “swirl” pattern that connects to a micron-sized iron sulfide at upper left surface of the spherule (Fig. 1a-c). Sulfur was detected in the vicinity of Fe-rich inclusions, and high-magnification EDS mapping reveals that sulfur forms rims around Fe-rich inclusions. A trace amount of Ni was also detected in the inclusions. High-resolution TEM images of the inclusions (Fig. 2) show crystal lattice fringes in the sulfur-bearing phase. Large Fe-rich inclusions (~100 nm) have sulfur-bearing rims

with a gap at the interface which implies volume reduction of the Fe-rich phase upon cooling. According to the EDS analysis at high magnification, the Fe-rich phase is Fe-Ni metal and the sulfur-rich rims are FeS.

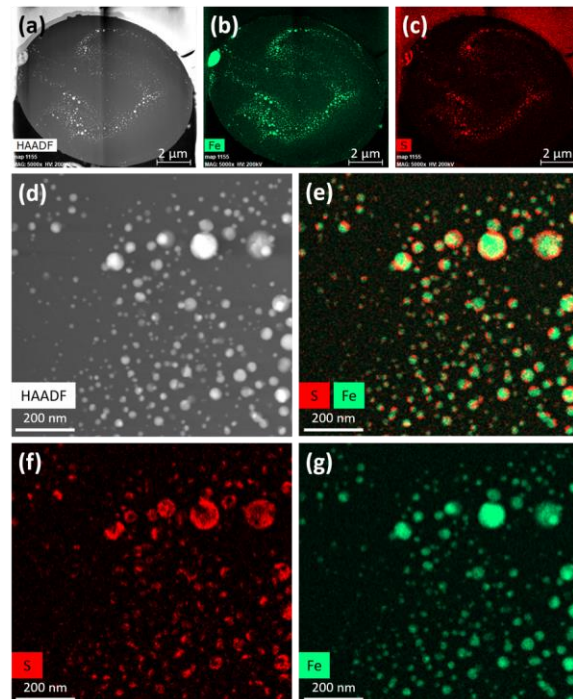


Fig. 1 HAADF images and EDS elemental maps of a silicate spherule with Fe-rich inclusions from lunar regolith 10084. (a) Low magnification HAADF image, (b) Fe map, (c) S map, (d) High magnification HAADF image, (e) Overlaid S and Fe maps showing S-rich rims on Fe particles, (f) S map, and (g) Fe map.

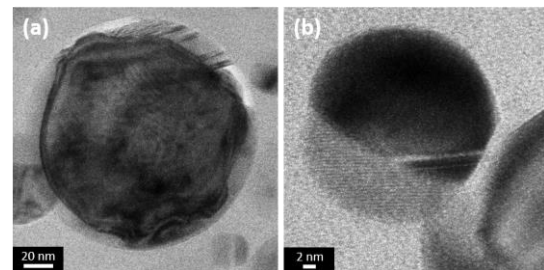


Fig. 2 S/TEM images of Fe-rich inclusions with crystalline iron sulfide on the surface (a) Large Fe-rich inclusion with a sulfide rim (b) small Fe-rich inclusion with sulfide on the surface.

The presence of FeS-rimmed metal in a “swirl” clearly distinguishes the Fe-rich inclusions observed in this study from previously proposed mechanisms for formation of npFe⁰ particles of condensation from vapor or reduction of higher valence Fe. One possible

route for the formation of FeS-rimmed Fe metal nanoparticles is impact melting in a reducing environment of $\text{Fe}_{(1-x)}\text{S}$ that was likely originally associated with the surface of the impacting micrometeorite. Formation of sulfide rims and metal cores due to impact melting has been reported in comet 81P/Wild 2 returned samples and in chondrites [10,11], and small melt droplets with immiscible metal-sulfide blebs have been reported on Itokawa regolith grains [12]. Sulfur-bearing Fe nanoparticles attributed to condensed vapor have also been reported in Itokawa regolith [13], but the morphology and the distribution do not resemble those in our samples. The spherical shape of the Fe-rich inclusions (Fig. 2) suggests that within the impact-generated glass melt droplet, immiscible molten sulfide partially decomposed and dispersed before quenching with a FeS rim. The “swirl” of inclusions from the surface sulfide suggests that the glassy spherule remained molten long enough for some internal mixing to occur but cooled fast enough to quench in amorphous structure. Since there is diurnal heating up to $\sim 400\text{K}$ on the surface of the Moon [14], even if FeS initially solidifies as an amorphous phase, the FeS phase should eventually crystallize with repeated heating cycles.

Fig. 3 shows another example of an amorphous silicate spherule with inclusions. In this case, a large single-crystal chromite inclusion ($3\text{-}4\mu\text{m}$ across) has spheroidal Fe particles along its rim, and they seem as if they buoyantly rose out of the surface of the chromite.

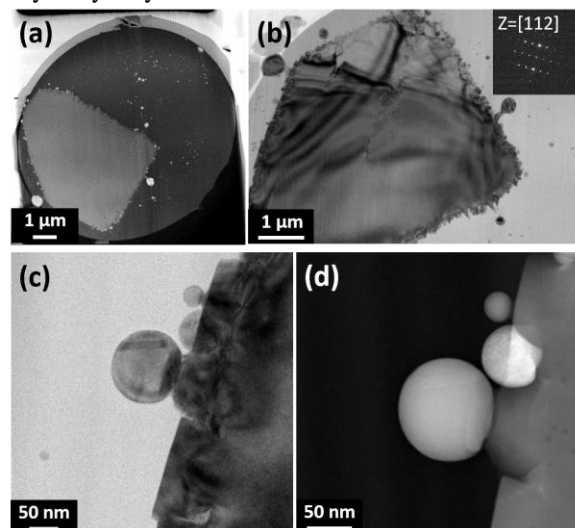


Fig. 3 S/TEM images of amorphous silicate spherule with a chromite inclusion (a) low magnification dark field STEM image (b) TEM image of chromite inclusion (insert: electron diffraction of chromite on [112] zone axis) (c) TEM image and (d) HAADF image of Fe spheres at the chromite surface. High contrast indicates the spheres are Fe-rich and lacking S-rich rims. A trace small amount of S was also detected in the large iron particles by EDS. It is unlikely that the Fe

was exsolved from the chromite crystal when the spherule formed because the HAADF image (Fig. 3a) does not show a gradient in contrast due to changing composition at the rim of the chromite.

The rough edges of the chromite crystal are an interesting feature. The lack of compositional difference suggests they are not due to irradiation. Instead, they may be due to partial melting and recrystallization of the surface. Since the Fe spheres in this glassy spherule do not have sulfur rims (Fig. 3c), they likely did not form from decomposition of sulfide. Instead, it is plausible that pre-existing Fe at the rim of the chromite crystal, perhaps in a rim formed by prior sputter and/or vapor deposition, aggregated into immiscible droplets within the molten silicate droplet as the impact formation of the glassy spherule incorporated the lunar chromite crystal.

Conclusion: Fe-rich inclusions in amorphous silicate spherules in lunar soil were characterized with S/TEM and EDS. Crystalline FeS rims at the surface of Fe-rich inclusions were observed in one silicate spherule. In the second silicate spherule with a chromite inclusion, Fe-rich particles were associated with the surface of the chromite and might originate from pre-existing npFe^0 on the surface of chromite prior to the impact that generated the glassy spherule. It is evident that Fe-rich particles seen in the interior of the spherules cannot form without the impact melting process, and the presence of FeS can be a criteria to determine the source of Fe. Since the inclusions (Fe and S) remained spherical but crystallized, we speculate that there was subsequent annealing sufficiently gentle that the amorphous silicate matrix was not disturbed. The composition and size of the FeS spherules could affect the optical properties differently than npFe^0 alone.

References: [1] Keller, L.P. & McKay, D.S. *GCA* **61**, 2331–2341 (1997); [2] Gu, L. *et al.* *Icarus* **303**, 47–52 (2018); [3] Basu, A. *J. Earth Syst. Sci.* **114**, 375–380 (2005); [4] Hapke, B. *The Moon* **7**, 342–355 (1973); [5] Housley, R.M. *et al.* *LPSC* **4**, 2737–2749 (1973); [6] Wang, K. *et al.* *EPSL* **337–338**, 17–24 (2012); [7] Chao, E.C. *et al.* *JGR* **75**, 7445–7479 (1970); [8] Burgess, K.D. and Stroud, R.M. *JGR Planets* **123**, 2022–2037 (2018); [9] Delano J.H. *LPSC* **91** D201-213 (1986) [10] Ishii H.A. *et al.* *Sci.* **319**, 447–450 (2008); [11] Scott E.R.D. *GCA* **46**, 813–823 (1982); [12] Keller L.P. & Berger E.L. *EPS* **66** 71 (2014); [13] Noguchi, T. *et al.* *Sci* **333** 1121–24 (2011); [14] Williams J.P. *et al.* *Icarus* **283** 300–325 (2017).

Acknowledgments: This research is supported by NASA grant NNX14AI48G to HAI. Thanks to K. Bustillo for technical support at the Molecular Foundry, which is supported by the Office of Science, BES, U.S. DOE, under Contract No. DE-AC02-05CH11231.